Using WSR-88D Data and Insolation Estimates to Determine Convective Boundary Layer Depth

KIMBERLY L. ELMORE

Cooperative Institute for Mesoscale Meteorological Studies, University of Oklahoma, and NOAA/National Severe Storms Laboratory, Norman, Oklahoma

PAMELA L. HEINSELMAN AND DAVID J. STENSRUD

NOAA/National Severe Storms Laboratory Norman, Oklahoma

(Manuscript received 1 March 2011, in final form 3 October 2011)

ABSTRACT

Prior work shows that Weather Surveillance Radar-1988 Doppler (WSR-88D) clear-air reflectivity can be used to determine convective boundary layer (CBL) depth. Based on that work, two simple linear regressions are developed that provide CBL depth. One requires only clear-air radar reflectivity from a single 4.5° elevation scan, whereas the other additionally requires the total, clear-sky insolation at the radar site, derived from the radar location and local time. Because only the most recent radar scan is used, the CBL depth can, in principle, be computed for every scan. The "true" CBL depth used to develop the models is based on human interpretation of the 915-MHz profiler data. The regressions presented in this work are developed using 17 summer days near Norman, Oklahoma, that have been previously investigated. The resulting equations and algorithms are applied to a testing dataset consisting of 7 days not previously analyzed. Though the regression using insolation estimates performs best, errors from both models are on the order of the expected error of the profiler-estimated CBL depth values. Of the two regressions, the one that uses insolation yields CBL depth estimates with an RMSE of 208 m, while the regression with only clear-air radar reflectivity yields CBL depth estimates with an RMSE of 330 m.

1. Introduction

Accurate convective boundary layer (CBL) depth estimates are required by fire weather forecasters (Clements et al. 2007) and when forecasting for air pollution and hazardous materials release (Dabberdt et al. 2004). CBL depth estimates are also important to convective initiation forecasts (Johnson and Mapes 2001; Browning et al. 2007) because the CBL depth is related to the strength of the capping inversion. For the various applications noted above, CBL estimates need to be available in near–real time. Accurate estimates of CBL depth are available from rawinsondes, but the rawinsonde network provides poor spatial and temporal resolution. Unfortunately, current numerical model estimates of CBL depth can be in error by as much as a factor of 2 (Grimsdell and Angevine 1998; Bright and Mullen 2002; Stensrud and Weiss 2002), which limits their utility.

White (1993) and Angevine et al. (1994) provide examples of CBL depth estimates from 915-MHz [very high frequency (VHF)] profilers. Recently, Bianco and Wilczak (2002) and Bianco et al. (2008) have developed automated algorithms to estimate CBL depth from VHF profilers. Unfortunately, these instruments are used primarily for air pollution research, making them unevenly distributed across the nation and unavailable in most areas. VHF profilers operate by detecting fluctuations in refractive index (C_n^2) near the top of the CBL. The same principles by which VHF profilers can detect the top of the CBL also apply to microwave radars, and there is an extensive history of prior work demonstrating that S-band radars possess sensitivity to C_n^2 fluctuations in the clear-air convective boundary layer (Hicks and Angell 1968; Hardy and Ottersen 1969; Konrad 1970; Doviak and Zrnic 1984; Browning et al. 2007). Thus, microwave weather radars, and in particular S-band weather radars, can detect clear-air returns. As shown by Lhermitte (1966), Konrad (1970), Gossard et al. (1984), Fairall (1991), and Wilson et al. (1994), S-band radars can also detect the interface associated with the top of the CBL.

Corresponding author address: Dr. Kimberly L. Elmore, NSSL, 120 David L. Boren Blvd., Norman, OK 73072.
E-mail: kim.elmore@noaa.gov

DOI: 10.1175/JTECH-D-11-00043.1

Heinselman et al. (2009, hereafter H09) have demonstrated that the S-band Weather Surveillance Radar-1988 Doppler (WSR-88D) radar can be used to determine the depth of the CBL on clear days during the summer in Oklahoma. H09 did their analysis by hand, and their results are in good agreement with 915-MHz profiler estimates of CBL depth. Because WSR-88Ds are deployed across the United States, the ability to routinely determine CBL depth with these radars would greatly increase the number of CBL depth observations.

Performing the analysis by hand on a routine basis is intractable operationally, but an automated method would provide far more frequent CBL depth estimates compared to other operational platforms. Automated CBL depth estimates could be available as often as every 5 min in real time from WSR-88D radar, depending upon the operating mode of the radar. Although these radar data would not solve the problem of spatially sparse CBL estimates, they would provide CBL depth estimates from across the nation and could be assimilated into various short-term forecast products and numerical models to provide improved analyses and model initial conditions. Clearly, to take full advantage of WSR-88D data, some sort of automated process is needed.

To that end, two linear models for calculating CBL depth are developed from the original 17 days of the Twin Lakes, Oklahoma (KTLX) WSR-88D data used in H09. These models are validated against 7 days that are not used in the H09 study. The data and experimental approach are found in section 2. The development of the linear model is discussed in section 3, results are discussed in section 4, while section 5 draws conclusions and proposes future work.

2. Data and experimental approach

The WSR-88D radar and the 915-MHz profiler are similar in that both can, in principle, provide reliable estimates of CBL depth on clear days (Lhermitte 1966; Konrad 1970; Gossard et al. 1984; Fairall 1991; Wilson et al. 1994). Hence, all of the days chosen for this analysis are mostly clear. The radar and profiler data used are from 2004 and all radar data are from the operational Twin Lakes (KTLX) radar. The days used as training and testing data appear in Table 1. All 7 days that are used for testing are chosen a priori subject to the following three requirements: 1) VHF profiler data are available, 2) there is not significant cloud cover, and 3) there is no precipitation. These days constitute all of the available data that meet the three preceding criteria. Because the radar data were collected in 2004, the Open Radar Data Acquisition system (Crum et al. 1998; Patel and Macemon 2003; Ice et al. 2004; Lee 2004; Ice et al. 2005) was not yet in use, and so the signal-to-noise ratio (SNR) is not available from the WSR-88D. Thus, radar reflectivity is used to determine the CBL depth, just as in H09. This is in direct contrast to the 915-MHz profilers, which use SNR for directly measuring the depth of the CBL.

TABLE 1. Days for which both radar and profiler data are available (all are for the year 2004).

Training data	Testing data
3 Jun	14 Jun
23 Jun	8 Jul
24 Jun	10 Jul
11 Jul	15 Jul
12 Jul	19 Jul
13 Jul	1 Aug
14 Jul	2 Aug
20 Jul	
21 Jul	
22 Jul	
26 Jul	
27 Jul	
3 Aug	
17 Aug	
18 Aug	
24 Aug	

For the profiler used here, CBL depth is determined subjectively by an expert as in Bianco and Wilczak (2002) and Bianco et al. (2008). This method avoids contamination by artifacts, such as ground clutter, and anomalous returns from birds, insects, aircraft, and clouds. There is uncertainty in the profiler estimates of the CBL depth, though that uncertainty is difficult to quantify. For the purposes of comparison, this uncertainty is assumed to be within $\pm$two pulse volumes, which is about $\pm$120 m. This choice is based on Bianco et al. (2008), where the RMS difference between the CBL depth, as determined independently by two experts, is 105 m. The CBL depth based on the profiler data in this study are available every 30 min.

Radar data are available approximately every 5 min, though only scans every 30 min are used for regression and testing to avoid overfitting resulting from serial correlation in the residuals. Also, data are taken at elevation angles of either 4.3° or 4.5°, depending upon the operating mode of the radar. The height of the radar observation is computed using a $\frac{4}{3}$ Earth radius correction [see Eq. (2.28d) of Doviak and Zrnic 1984]. As shown in H09, the radar CBL top is represented by a reflectivity ring centered on the radar, with the ring moving outward (upward) as the CBL deepens. The enhanced return from the CBL eventually vanishes at the end of the day as insolation decreases and the CBL collapses. Because these radar data are inherently noisy, the data at each range are averaged over the full 360° circle. This differs from the

approach used in H09, where the data are averaged over octants. The data are then interpreted as a vertical reflectivity profile (VRP). However, even after averaging over the full 360°, the radar data are still noisy. Thus, a final smoothing is performed on the VRP using a smoothing spline (Hastie and Tibshirani 1990). This final step usually results in a single, coherent peak within the vertical reflectivity profile.

As in H09, there is occasionally a residual layer that is left over from the previous day's CBL. This residual layer can sometimes generate a stronger return than that generated by the top of the real CBL, resulting in multiple peaks in the VRP. The existence of multiple peaks requires a coherency check to limit large anomalous variations in CBL depth over short time intervals. Because the CBL is driven by insolation, its depth in the morning is very shallow (defined here as 100 m) and increases essentially (but not strictly) monotonically as the day wears on. Hence, to start the process, any early morning reflectivity peaks (up to about 3 h after sunrise) above 100 m are ignored.

During the first 4 h after sunrise, the VRP peak representing the CBL depth and used in the linear regression model is assumed to be the peak at the lowest altitude. As time progresses and the CBL deepens, other peaks may exist in the reflectivity profile, but only the peak closest to the prior peak is used based on a continuity constraint. Occasionally, no peak is found and so the height of the VRP peak is assumed to be unchanged from the prior value. In other cases, a spurious peak is found, where spurious is defined as a peak of more than 750-m height difference from the prior value (the continuity constraint). Spurious peaks are ignored, leaving the height of the VRP peak also unchanged from the prior value. Spurious peaks are common, though typically last only 20–30 min.

The height of the VRP peak is not the only statistic gleaned from the radar data and tested in the linear regression. Other values are derived, including the maximum reflectivity within the layer of useful clear-air return; the reflectivity at the top, bottom, and center of the layer; the thickness of the layer; and also the mean and median reflectivity within the layer. A radar-independent parameter is constructed from the integrated total clear-sky insolation since sunrise (kJ m^{-2}), which is calculated using the location of the radar site. Because no pyranometers are used operationally at the radar site the insolation is not measured, but instead the maximum available solar radiation is used. Total integrated insolation is investigated because insolation drives the CBL development. In practice, insolation values can be measured either directly or through numerical forecast models, thereby providing reasonable insolation values even under non-clear-sky conditions. All of these parameters (and their squares) are investigated as predictors. The independent (predicted) parameter is the CBL depth based on manual inspection of the profiler data; the profiler data are considered to be ''truth.''

3. Model selection

A linear model is always a good starting point because it is convenient, simple, and accommodates straightforward model selection. This is especially true when there are only a few predictors to consider, as in the current case. Bootstrap model selection [also called bootstrap validation; see Efron and Tibshirani (1993, 1995) and Davison and Hinkley (1999)] is used to estimate the generalization or expected prediction error. The model with the smallest expected prediction error, subject to overfitting concerns, is tested. Bootstrap resampling uses observations from the training data, selected at random and *with replacement.* Each resampled dataset is termed a bootstrap replicate. Bootstrap resampling is a subset of Monte Carlo techniques and is used to nonparametrically characterize the uncertainty that is inherent in data samples.

Bootstrap validation proceeds identically to standard cross validation, except that bootstrap validation repeatedly fits a given model on bootstrap replicates, and then calculates prediction error estimates from these bootstrap fits. In this case, once a replicate is assembled from the available observations, a regression model is fit and the prediction error of the model is calculated. The process of assembling a bootstrap replicate and then fitting the regression model to it is repeated 5000 times in order to provide good empirical confidence interval estimates for both the prediction error and the regression coefficients. The resulting bootstrap mean prediction error estimates offer a generally more accurate representation of expected model performance than either the sample prediction error of the model fitted to the original dataset or cross-validation techniques (Efron and Tibshirani 1993, 1995; Davison and Hinkley 1999).

Two models are developed: the first is restricted to only radar-observable input, but the second model is unrestricted in the scope of available predictors. For both models, all possible single-parameter models are investigated first (Fig. 1). For the radar-only models, insolation terms are excluded. Once the best performing single-parameter model is identified it is retained, and all remaining parameters are examined to determine the best performing two-parameter model. This forward selection process continues until either all parameters are used or the addition of a new parameter provides no further benefit.

Following this procedure, the linear model for determining CBL depth using radar data plus insolation uses

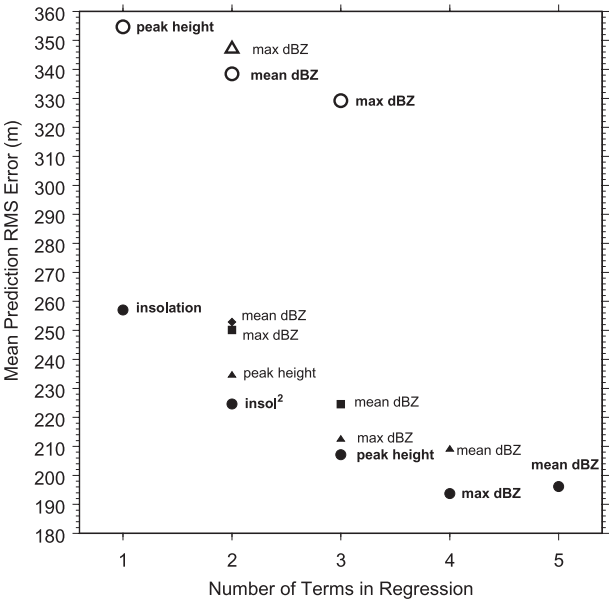

FIG. 1. The RMS prediction errors for the training set. Each symbol represents the addition of a different predictor (noted to the right of the symbol) and the associated RMS error. Models that use reflectivity only (open symbols) and include insolation (filled symbols) are shown. For models that use only reflectivity, the best single-term model uses the height of the peak reflectivity (peak height). The best two-term model uses peak height + the mean reflectivity in the enhanced layer; the only available three-term model includes the maximum reflectivity in the enhanced layer. For models that include insolation, the best single-term model simply uses insolation only. Of the possible two-term models the best adds $(\text{insolation})^2$ to insolation. The best three-term model adds peak height to the insolation + $(\text{insolation})^2$ model, and so on. Expected prediction errors are based on bootstrap resampling.

the following three or four terms: total insolation, total insolation squared, the height of the peak radar reflectivity, and the maximum radar reflectivity (Fig. 1). The addition of a fifth term (mean reflectivity) clearly deteriorates the model performance, and thus is not included. A similar pattern emerges for the multiple R^2 (the coefficient of determination) for the best performing models when plotted against the number of predictors (not shown). Only one predictor, the height of the VRP peak, is used for the radar-only model. For the model utilizing insolation, only three terms are used. For both models, the number of terms is truncated to avoid overfitting the model to training data.

The resulting regression equations for CBL depth are given by

$$D = 0.0757 + 0.9905(H), \tag{1}$$

and

$$D = -0.1192 + 6.856 \times 10^{-5}(I) - 8.710 \times 10^{-10}(I^2) + 0.2888(H), \tag{2}$$

where D is the depth (km) of the CBL, H is the height of the VRP peak (km), I is the total insolation since sunrise (kJ m^{-2}), and I^2 is the total insolation since sunrise squared. All radar parameters are mean values taken over 360° at either 4.3° or 4.5° elevation, depending upon the radar mode. In Eq. (2) insolation is used as a second-order predictor—one term is first order and the other is second order; hence, the model is second-order linear for insolation only. No other second-order terms performed well.

Bootstrap resampling is employed to determine if the regression coefficients are significant at $p = 0.05$. Except for the intercept term, which is always "significant," the regression coefficients are deemed statistically different from zero if the confidence interval describing them does not contain zero. The 2.5 and 97.5 percentiles for Eqs. (1) and (2) are given respectively in Table 2. In all cases, the regression coefficients are statistically significant at $p = 0.05$.

All of these predictors are physically interpretable. The two insolation terms are functional rather than observed because the equation is derived for days that are essentially cloudless. Insolation is included because it drives the CBL. Insolation is also included as a second-order term because inspection (Fig. 2) reveals that the CBL depth responds as the square of total insolation. The height of the peak radar reflectivity (Fig. 2) is the basis of H09 and is an obvious choice because the interface between the CBL and the stable atmosphere generates the radar return (Rabin and Doviak 1989; Doviak and Zrnic 1984), similar to what VHF profilers detect. Thus, its height should be a good indicator of CBL depth.

TABLE 2. Regression coefficient 95% empirical bootstrap confidence limits.

	Intercept		I		I^2		H	
	2.5%	97.5%	2.5%	97.5%	2.5%	97.5%	2.5%	97.5%
Eq. (1)	−0.1506	0.0698	—	—	—	—	0.9713	1.1545
Eq. (2)	−0.1758	−0.0748	6.132×10^{-5}	7.595×10^{-5}	-1.073×10^{-9}	-6.764×10^{-10}	0.2057	0.3828

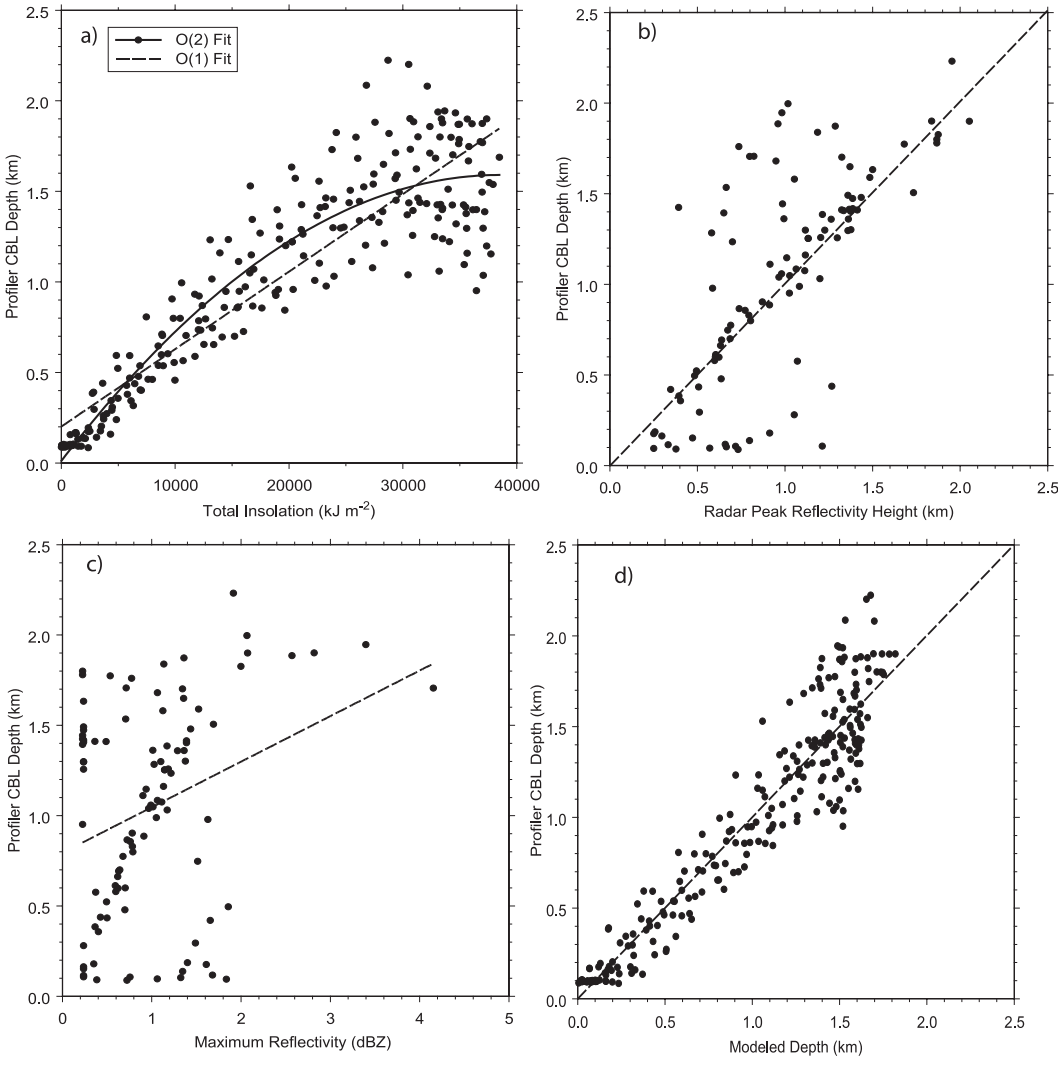

FIG. 2. Plots of individual variables against the CBL depth as determined by a 915-MHz profiler. Shown are (a) the CBL depth as a function of insolation alone show a first- (dashed lines) and second-order (dotted lines) regression fit; (b) the CBL depth based on the height of the peak radar reflectivity alone, where the first-order regression fit (dashed line) is shown; (c) the CBL depth as a function of the peak reflectivity alone [the first-order regression fit is shown (dashed line)]; and (d) shows the model CBL depth against the measured CBL depth, all for the training data (dashed line is a 1:1 line, not a regression fit).

Statistics associated with some of the typical predictor selection techniques, such as t statistics, F statistics, etc., indicate that retaining the maximum dBZ as a fourth predictor may be justified (Fig. 2). The physical interpretation of maximum reflectivity is less certain. Clear-air return originates within strong gradients of refractive index, caused in part by large gradients in temperature and moisture. These gradients may be maximized after the residual layer has been entrained into the CBL. Such entrainment would occur late in the day and may indicate strong mixing. Perhaps insects become more active and numerous as the CBL deepens, leading to a biogenic increase in reflectivity at the top of the CBL. Regardless of the cause, retaining the maximum reflectivity term does not improve the performance of the model by a significant amount and may result in overfitting. Thus, this predictor is not used in (2).

4. Results

Figure 3 shows model performance for a specific test day, 14 June 2004. Even though both the radar-only model and the three-term model that includes insolation do well in capturing the increasing depth of the CBL as the day progresses, the three-term model is more accurate. When the three-term model performance is

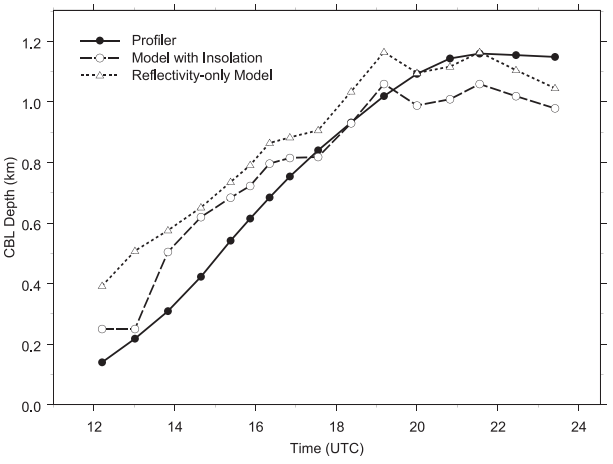

FIG. 3. Model CBL depth estimates compared to VHF profiler CBL depth estimates for both the radar-only model and the three-term model that includes insolation. The VHF profiler estimates (solid line with dots), the radar-only model (dotted line with open triangles), and the three-term model that includes an insolation estimate (dashed line with open circles) are shown.

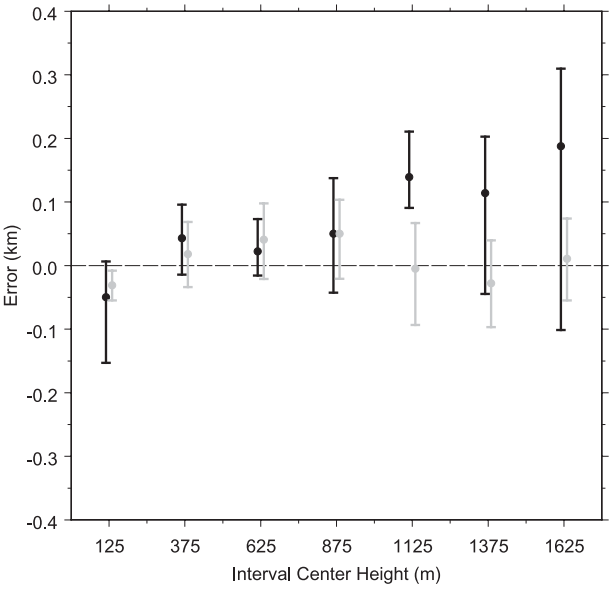

FIG. 4. The 95% confidence limits based on bootstrap tilting for CBL depth three-term model compared to CBL depth based on VHF profiler data. The error is defined as $CBL_{radar} - CBL_{profiler}$, and the error bars are computed using bootstrap tilting. Training data (gray bars) and testing data (black bars) are shown. Where the error bars overlap the zero line, the model error is not statistically different form 0 with 95% confidence.

stratified by height, both the training and testing datasets yield good results (Fig. 4). As is almost always the case, the fitted model performs better on the training data than on the testing data. Except for the lowest height interval centered on 125 m, the 95% bootstrap confidence intervals for the training data errors all are statistically indistinguishable from zero. This means that for the training data, the linear regression model performance is statistically indistinguishable from the CBL depth measured with the profiler. However, the 95% confidence intervals for the testing data do not always contain zero. This indicates that for the testing data, there is a statistical difference between the CBL depth determined by the model and that determined from the radar.

However, the profiler CBL depth also contains some uncertainty. Even though there is no CBL depth estimate independent from the profiler, the profiler estimate itself possesses some uncertainty. This uncertainty may be from one to as many as three gate spacings, depending upon the human interpretation of the maximum SNR height, in line with Bianco et al. (2008), who found 105-m RMS uncertainty between expert human estimates. The profiler has a gate spacing of 60 m for this work, so the bias errors in the CBL depth determined from both models are on the order of the uncertainty within the profiler CBL depth estimates (Fig. 4, only three-term model shown). If the regression model uses only radar data, then the results are worse. Finally, errors for the three-term model are only about twice the value of the RMS difference between different experts estimating CBL depth by hand (Bianco et al. 2008).

5. Conclusions

Both simple regression schemes to determine the depth of the CBL from the KTLX radar perform well, though the model that uses insolation is considerably better, with an RMSE of about 207 m. The best radar-only model results in a RMSE of roughly 330 m. The terms contained in the model that uses insolation are physically reasonable, interpretable, and include first- and second-order terms that describe the physical process driving the convective boundary layer (insolation). However, one drawback is that the generality of this particular formulation, developed over one summer in central Oklahoma, is understandably suspect. Adding radar peak reflectivity height to the insolation makes a modest improvement, decreasing the RMSE by about 18 m, from 225 to 207 m. Many terms that cannot be easily measured also have a strong effect on CBL depth. Chief among them may be the partitioning between sensible and latent heat flux at the ground surface. However, in other areas, such as desert, heavily wooded regions, swampy regions, or prairie grasslands, the flux partitioning is likely to be different. If the flux partitioning is different, then the same terms probably appear in the regression, but with different coefficients. To test the generality of this algorithm, a similar study needs be done where vegetation and rainfall patterns

differ significantly from those in central Oklahoma during the summer. Direct observations of insolation or even forecasts of insolation from numerical model forecasts may be helpful on days with more cloudy conditions in order to more accurately diagnose CBL depth. If the particular regression developed in this work does not generalize to ecologically different regions, then perhaps sensible heat flux forecasts could be used in place of the insolation estimate, though doing so requires redevelopment of the regression equations and testing. If only the height of the peak reflectivity is used then accuracy suffers, but such a model may generalize to different regions better than the model that includes insolation. Considering that numerical forecast model CBL depths can be in error by as much as factor of 2, radar-derived CBL depth estimates that are off by only ~300 m would be enormously helpful if available across the nation.

Acknowledgments. This work was supported by the NEXRAD Product Improvement Program, by NOAA/Office of Oceanic and Atmospheric Research under NOAA–University of Oklahoma Cooperative Agreement NA17RJ1227, U.S. Department of Commerce and the University of Oklahoma Cooperative Institute for Mesoscale Meteorological Studies. The statements, findings, conclusions, and recommendations are those of the authors and do not necessarily reflect the views of NOAA, the U.S. Department of Commerce, or the University of Oklahoma.

REFERENCES

Angevine, W. M., A. B. White, and S. K. Avery, 1994: Boundary-layer depth and entrainment zone characterization with a boundary-layer profiler. *Bound.-Layer Meteor.,* **68,** 375–385.

Bianco, S., and J. M. Wilczak, 2002: Convective boundary layer depth estimation from wind profilers: Statistical comparison between an automated algorithm and expert estimations. *J. Atmos. Oceanic Technol.,* **19,** 1745–1758.

——, ——, and A. B. White, 2008: Convective boundary layer depth: Improved measurement by Doppler radar wind profiler using fuzzy logic methods. *J. Atmos. Oceanic Technol.,* **25,** 1397–1413.

Bright, D. R., and S. L. Mullen, 2002: The sensitivity of the numerical simulation of the southwest monsoon boundary layer to the choice of PBL turbulence parameterization in MM5. *Wea. Forecasting,* **17,** 99–114.

Browning, K. A., and Coauthors, 2007: The convective storm initiation project. *Bull. Amer. Meteor. Soc.,* **88,** 1939–1955.

Clements, C. B., and Coauthors, 2007: Observing the dynamics of wildland grass fires: FireFlux – A field validation experiment. *Bull. Amer. Meteor. Soc.,* **88,** 1369–1382.

Crum, T. D., R. E. Saffle, and J. W. Wilson, 1998: An update on the NEXRAD program and future WSR-88D. *Wea. Forecasting,* **13,** 253–262.

Dabberdt, W. F., and Coauthors, 2004: Meteorological research needs for improved air quality forecasting: Report of the 11th prospectus development team of the U.S. Weather Research Program. *Bull. Amer. Meteor. Soc.,* **85,** 563–586.

Davison, A. C., and D. V. Hinkley, 1999: *Bootstrap Methods and Their Applications*. Cambridge University Press, 582 pp.

Doviak, R. J., and D. S. Zrnic, 1984: *Doppler Radar and Weather Observations*. Academic Press, 458 pp.

Efron, B., and R. J. Tibshirani, 1993: *An Introduction to the Bootstrap*. Chapman and Hall, 436 pp.

——, and ——, 1995: Cross validation and the bootstrap: Estimating the error rate of a prediction rule. Stanford Tech. Rep. 176, 28 pp. [Available online at http://statistics.stanford.edu/~ckirby/techreports/BIO/BIO%20176.pdf.]

Fairall, C. W., 1991: The humidity and temperature sensitivity of clear-air radars in the convective boundary layer. *J. Appl. Meteor.,* **30,** 1064–1074.

Gossard, E. E., R. B. Chadwick, T. P. Detman, and J. Gaynor, 1984: Capability of surface-based clear-air Doppler radar for monitoring meteorological structures of elevated layers. *J. Climate Appl. Meteor.,* **23,** 474–485.

Grimsdell, A. W., and W. M. Angevine, 1998: Convective boundary layer height measurement with wind profilers and comparison to cloud base. *J. Atmos. Oceanic Technol.,* **15,** 1331–1338.

Hardy, K. R., and H. Ottersen, 1969: Radar investigations of convective patterns in the clear atmosphere. *J. Atmos. Sci.,* **26,** 666–672.

Hastie, T. J., and R. J. Tibshirani, 1990: *Generalized Additive Models.* Chapman and Hall, 535 pp.

Heinselman, P. L., D. J. Stensrud, R. M. Hluchan, P. L. Spencer, P. C. Burke, and K. L. Elmore, 2009: Radar reflectivity–based estimates of mixed layer depth. *J. Atmos. Oceanic Technol.,* **26,** 229–239.

Hicks, J. J., and J. K. Angell, 1968: Radar observations of breaking gravitational waves in the visually clear atmosphere. *J. Appl. Meteor.,* **7,** 114–121.

Ice, R. L., R. D. Rhoton, D. S. Saxion, N. K. Patel, D. Sirmans, D. A. Warde, D. L. Rachel, and R. G. Fehlen, 2004: Radar Operations Center (ROC) evaluation of the WSR-88D open radar data acquisition (ORDA) system signal processing. Preprints, *20th Int. Conf. on Interactive Information and Processing Systems for Meteorology, Oceanography, and Hydrology,* Seattle, WA, Amer. Meteor. Soc., 5.5. [Available online at http://ams.confex.com/ams/pdfpapers/70692.pdf.]

——, and Coauthors, 2005: Radar Operations Center (ROC) evaluation of new signal processing techniques for the WSR-88D. Preprints, *21st Int. Conf. on Interactive Information and Processing Systems for Meteorology, Oceanography, and Hydrology,* San Diego, CA, Amer. Meteor. Soc., P1.4. [Available online at http://ams.confex.com/ams/pdfpapers/85859.pdf.]

Johnson, R. H., and B. E. Mapes, 2001: Mesoscale processes and severe convective weather. *Severe Convective Storms, Meteor. Monogr.,* No. 50, Amer. Meteor. Soc., 71–122.

Konrad, T. G., 1970: The dynamics of the convective process in clear air as seen by radar. *J. Atmos. Sci.,* **27,** 1138–1147.

Lee, R. R., 2004: WSR-88D open radar data acquisition (ORDA) algorithm evaluations. Preprints, *32nd Conf. on Radar Meteorology,* Albuquerque, NM, Amer. Meteor. Soc., P8R.8. [Available online at http://ams.confex.com/ams/pdfpapers/96604.pdf.]

Lhermitte, R. M., 1966: Probing air motion by Doppler analysis of radar clear air returns. *J. Atmos. Sci.,* **23,** 575–591.

Patel, N. K., and W. R. Macemon, 2003: NEXRAD Open Radar Data Acquisition (ORDA) signal processing and signal path. Preprints, *20th Int. Conf. on Interactive Information and Processing Systems for Meteorology, Oceanography, and Hydrology,* Seattle, WA, Amer. Meteor. Soc., 5.4. [Available online at http://ams.confex.com/ams/pdfpapers/70926.pdf.]

Rabin, R. M., and R. J. Doviak, 1989: Meteorological and astronomical influences on radar reflectivity in the convective boundary layer. *J. Appl. Meteor.,* **28,** 1226–1235.

Stensrud, D. J., and S. J. Weiss, 2002: Mesoscale model ensemble forecasts of the 3 May 1999 tornado outbreak. *Wea. Forecasting,* **17,** 526–543.

White, A. B., 1993: Mixing depth detection using 915-MHz radar reflectivity data. Preprints, *Eighth Symp. on Meteorological Observations and Instrumentation,* Anaheim, CA, Amer. Meteor. Soc., 248–250.

Wilson, J. W., T. M. Weckworth, J. Vivekanandan, R. M. Wakimoto, and R. W. Russel, 1994: Boundary layer clear-air radar echoes: Origin of echoes and accuracy of derived winds. *J. Atmos. Oceanic Technol.,* **11,** 1184–1206.